Evolution of Surface Morphology in 2-Hydroxyethyl Methacrylate Copolymer Exposed to γ Radiation

Kuo-feng Chou

Department of Biomedical Engineering,Yuanpei University of Science and Technology, Hsinchu, Taiwan

Sanboh Lee*

Department of Materials Science and Engineering, National Tsing Hua University, Hsinchu, Taiwan

Julie P. Harmon

Chemistry Department, University of South Florida, Tampa, Florida 33620-5250

Received October 28, 2002

ABSTRACT: Buckling patterns were observed on the outer surface of HEMA copolymers irradiated in air and subsequently immersed in solvents. The structure parameters of these buckling patterns on the irradiated copolymers were obtained via image analysis; these parameters include pattern size, pattern uniformity, and undulation amplification. The pattern size increased with time due to the release of elastic constraints and then reached a constant morphology, which persisted upon attaining equilibrium swelling due to a radiation-induced concentration gradient in carboxyl groups along the thickness direction. The pattern size increased as the dose rate decreased. Solution pH also influenced the surface morphology of irradiated samples. Increases in swelling accompanied by increasing the pH of the solvent resulted in patterns with morphologies, which shifted from noodlelike to needlelike grains. All of this is explained by the changes in osmotic pressure and radiation-induced cross-link density gradients along the thickness direction of the samples.

1. Introduction

Patterns observed on the surface of ionic polymer gels and swollen polymer films have been hypothesized to originate via one of two mechanisms.[1−10] Tanaka et al.[1,2] observed that buckling patterns formed on ionic polymer gel surfaces. They hypothesized that these patterns arose from mechanical instability induced by the interaction of high osmotic pressure with mechanical constraints induced during swelling. They also evaluated the size of the undulation structures based on the changes in the elastic deformation energy of the polymer gels during swelling. Similar buckling patterns were observed on polymer films coated on silicon substrates and immersed in different solvents.[11−17] In these studies, pattern formation was explained to originate from the action of long- and short-range forces among the solvent, film, and substrate. The authors correlated pattern size with the thickness of film and interaction parameters. On the other hand, Onuki,[6] Panyukov, and Rabin[7,9] attributed the formation of similar patterns to phase transitions. They proposed that a phase transformation occurs during polymer swelling. This phase transition is influenced by the elastic medium, such that an unstable pattern occurrence coincides with spinodal decomposition. In a previous study,[18,19] we reported that buckling patterns were obtained on the surface of irradiated HEMA copolymer after immersion in water or buffer solutions. In the research reported herein, we attempt to further study and explain these buckling patterns.

Numerous studies on the effects of radiation on polymer matrices led to a scenario, which explains complicated radiolysis products.[20−25] γ irradiation induces the formation of free radicals in the polymer matrix. Polymers formed from 1,1-disubstituted vinyl monomers have a tendency to undergo scission, whereas structures formed from monosubstituted vinyl compounds tend to undergo cross-linking. Free radicals also react with oxygen present in the system and are "quenched" undergoing reactions, which lead to the formation of various carbonyl-containing compounds. Interaction of the free radicals and other unstable radiolysis products with oxygen results in a complicated population of reaction products within the polymer matrix. When the oxygen present in the matrix during radiation is depleted by the quenching process, a new supply of oxygen slowly diffuses in from the outside forming a Fickian concentration gradient. This oxygen reacts with additional free radicals, resulting in a gradient in radiolysis products. Hence, the structure and the surface of a sample may vary significantly from that of the core.

This study is the first study that correlates characteristics of immersion-induced surface structure to γ irradiation and the pH of the buffer solution used for immersion. The experimental results are explained by gradients in radiation-induced scission products that result in swelling gradients, which result in buckling patterns.

2. Experimental Section

The soft contact lens blanks of HEMA copolymer were obtained from Canadian Soft Contact Lens Laboratories Ltd., Montreal, Quebec, Canada. The original samples were disks of 12.8 mm diameter and 6.0 mm thick. These materials were cut into slices and polished with 600 and 1200 grit emery papers followed by 1.0 and 0.05 μm Al_2O_3 slurries. A series of 1.4 and 1.2 mm thick, polished specimens were annealed in a vacuum oven at 60 °C for 7 days and slowly cooled to room temperature. Any residual stresses induced by machining were eliminated via annealing.

10.1021/ma021635g CCC: $25.00
Published on Web 06/25/2003

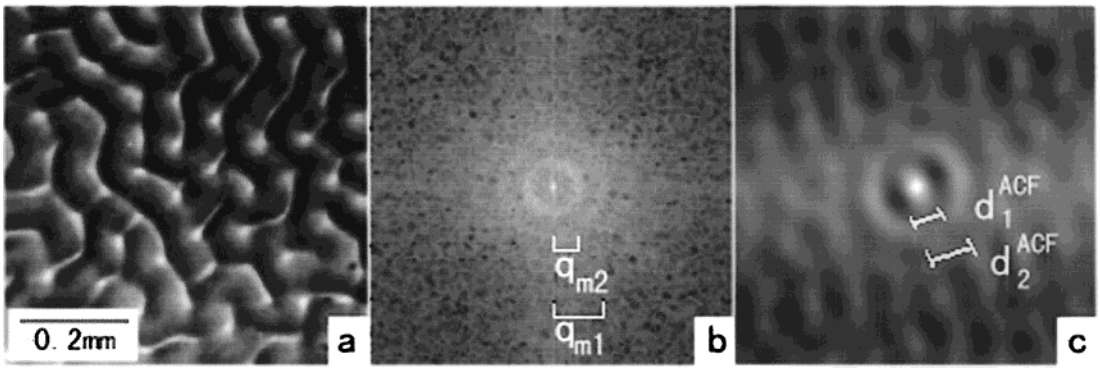

Figure 1. Image processing of patterns: (a) the origin surface pattern on specimen exposed to 200 kGy at a dose rate of 7.1 kGy/h and immersed in deionized water at 30 °C, (b) the FFT image of (a), and (c) the image after the ACF process.

The 1.2 and 1.4 mm thick specimens were exposed on γ-ray radiation in air via a 30 000 Ci cobalt-60 source at the Isotope Center of National Tsing Hua University. The 1.4 mm thick samples were exposed to total doses of 100, 200, 300, and 400 kGy at a constant dose rate of 7.1 kGy/h. These samples were then immersed in deionized water at 30 °C. One-half of 1.2 mm thick specimens were exposed to a total dose of 400 kGy at dose rates of 30, 21, 14.5, 10, and 6.5 kGy/h and then immersed in deionized water at 40 °C. The remaining 1.2 mm thick samples were irradiated at a dose rate of 14.5 kGy/h to a total dose of 300 kGy. These samples were immersed in 40 °C buffer solutions at pHs of 3.9, 4.8, 5.6, 6.5, 7.2, and 7.8. The buffer solutions were prepared by mixing anhydrous citric acid obtained from Tedia Co., Fairfield, OH, and anhydrous, dibasic sodium phosphate obtained from the Showa Chemicals Inc., Tokyo, Japan, with water. A Jenco Electronics digital pH meter was used to measure the pH of the buffers.

Morphological changes accompanying immersion were observed using an Olympus BH-2 optical microscope with an image capturing system. Images of the surface patterns were analyzed by Scion image analysis software developed by The National Institute of Health and modified by Scion Corp., Frederick, MD.

Specimens irradiated in nitrogen were used as controls in order to investigate the effect of oxygen on the formation of patterns. The specimens irradiated in air were cut into four layers from the surface to inner regions and ground into powder. The thickness of each layer was 0.1 mm. Each layer is ground into powders and mixed with 10 mL of deionized water, and then the pH of each solution was measured by a Jenco Electronics digital pH meter. Samples were titrated with 0.1 N NaOH solution until the equivalence points were reached. The NaOH solution was obtained from Fisher Scientific Co., Loughborough, UK. The concentrations of carboxyl groups in the powders were obtained by evaluating the consumption of NaOH solution during titration.[26] The glass transition temperature of each layer was measured by using Seiko SSC 5200 differential scanning calorimeter (DSC), Tokyo, Japan. The temperature was increased from 25 to 100 °C with the heating rate of 5 °C/min.

3. Results and Discussion

3.1. Effect of γ Radiation on Surface Morphology. As irradiated samples were immersed in water, buckling patterns appeared on the surfaces facing the γ source. The images of patterns are shown in Figure 1a. As in our previous studies,[18,19] the patterns appeared only on the specimens irradiated in air. Earlier measurements made in our laboratory demonstrated that the nonirradiated specimens and samples irradiated in a vacuum did not buckle upon immersion in solvents. The surfaces of samples irradiated in nitrogen remained smooth throughout the entire mass transport process. Swelling in the outer layers of the specimens irradiated in air was significantly different from that in the bulk region, and buckling patterns persisted after swelling was complete.

Table 1. Glass Transition Temperature (T_g) of Various Layers in HEMA Copolymer Irradiated by γ Ray at 400 kGy Where L Is the Central Position of Each Layer from the Surface along the Thickness Direction

L (mm)	0.05	0.15	0.25	0.35
T_g (°C)	68	67	67	66

Table 2. Concentrations (C_A in Units of 10^{-6} mol/g) of Carboxyl Groups in Various Layers of HEMA Copolymer Irradiated by γ Ray Where L Is the Central Position of Each Layer from the Surface along the Thickness Direction

	L (mm)			
dose (kGy)	0.05	0.15	0.25	0.35
0	0.39	0.39	0.39	0.39
100	1.38	1.33	1.32	0.76
200	1.74	1.72	1.62	1.52
300	7.63	3.25	2.57	1.67
400	33.9	4.3	1.12	0.76

The inhomogeneity between outer surface and inner layers is consistent with the explanation that oxygen diffuses from the outer surface to the HEMA copolymer when the specimens are irradiated in air. There are two hypotheses explaining the effect of oxygen on the formation of surface patterns. First, oxygen reacts with radicals and decreases the cross-link density. The cross-link density, then, increases with decreasing depth from the outer surface. During water uptake the outer surface is swollen first. The glass transition temperature decreases slightly with increasing depth from surface to inner layer of irradiated specimen as shown in Table 1 and is 65 °C regardless of depth in nonirradiated specimens. That means the cross-link density influences inhomogeneity but is not the major mechanism responsible for the pattern formation. The second hypothesis is that oxygen reacts with radicals to form carboxyl groups. We have previously shown that radiation induces the formation of acid functional carboxyl groups.[19] These acid groups lower the pH value of the water and induce swelling that increases with the radiation dose. The surface layers, which contain greater populations of these moieties, exhibit the highest degree of swelling. The concentration of carboxyl groups was determined by titration and is listed in Table 2. The results show that the concentration of carboxyl groups at the surface is several times greater than that in the inner layers. The difference in carboxyl content between outside layers and inner layers increases with irradiation dose. Earlier, we investigated the effect of oxygen diffusion via dose rate experiments. This earlier data and the

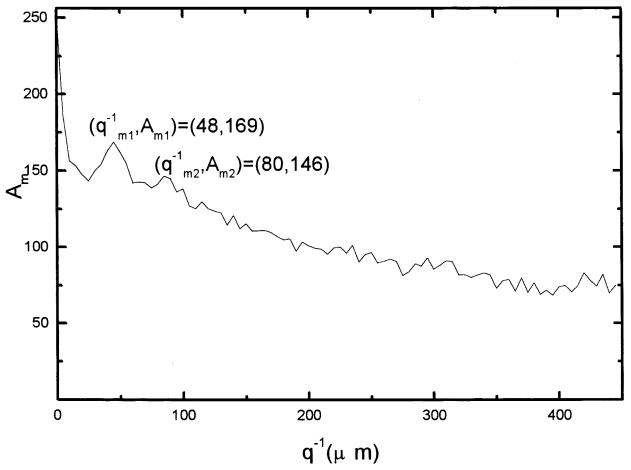

Figure 2. Curve of intensity vs q^{-1} corresponding to Figure 1b.

Table 3. Maxima in Pattern Structure Parameters of Specimens Exposed to Various Doses with Dose Rate 7.1 kGy/h and Immersed in Water at 30 °C

dose (kGy)	q_{max1}^{-1} (μm)	q_{max2}^{-1} (μm)	d_{max1}^{ACF} (μm)	d_{max2}^{ACF} (μm)	A_{m1}	I_H
100	48	80	46	78	138	43
200	52	86	50	81	168	221
300	55	89	56	86	159	161

data presented here are consistent with the interpretation, suggested by Tanaka et al.,[1,2] that the occurrence of buckled patterns results from the mechanical instability between the swollen outer layer and the fixed inner layer in the process of collective diffusion. Thus, also the mechanisms leading to periodic surface instabilities are not fully understood as present; it is tempting to speculate that, in the experiments described here, persistent mechanical swelling constraints are the origin of the surface morphologies.

3.2. Characteristic Parameters of Pattern and Image Processing. The structure parameters of these patterns were evaluated using Scion image processing software. First, images of the patterns were transformed into the frequency domain by fast Fourier transformation (FFT). In Figure 1b, two concentric circles of radii q_{m1} and q_{m2} are observed in the center of FFT images. The reciprocals of q_{m1} and q_{m2} (q_{m1}^{-1} and q_{m2}^{-1}) are termed the characteristic wavelengths of the short- and long-range regular structures. The values of q_{m1}^{-1} and q_{m2}^{-1} are evaluated from the position of peaks shown on the curve of intensity vs radius of the FFT image (Figure 2). The intensity of peak, assigned as A_m, is an index of pattern regularity. Note that the peak at $q_m^{-1} = 0$ is an artifact and has no physical meaning. The nonperiodic component of the image was filtered via an autocorrelation function. The image of the regular structure shown in Figure 2 was obtained by inversing the image into real space after the processing of the autocorrelation function. In Figure 1c, the periodic lengths of short- and long-range structures on the filtered image were measured and notated d_1^{ACF} and d_2^{ACF}, respectively. The gray level of the image pattern, I_H (the whole scale from white to black is divided into 256 levels), is obtained as the index of height of undulation.

3.3. Effect of Dose on Pattern Parameters. Samples irradiated to a dose of 300 kGy were immersed in water at 30 °C. Buckling patterns formed on surfaces of these samples are shown in Figure 3. The surface morphology changes with increasing immersion time. The texture variation is sinusoidal and similar to the undulation form observed previously in several studies on polymer films.[10−17] However, Tanaka et al.[1] and Hirohawa et al.[2] observed spike patterns rather than sinusoidal patterns on ionic polymer gels.

Plots of q_m^{-1}, d^{ACF}, A_m, and I_H vs time are shown in Figure 4. As seen in the q_m^{-1} plot, the characteristic wavelength increases to a maximum and then decreases as the extent of swelling increases. The difference between maximum and minimum of q_{m1}^{-1} and d_1^{ACF} is

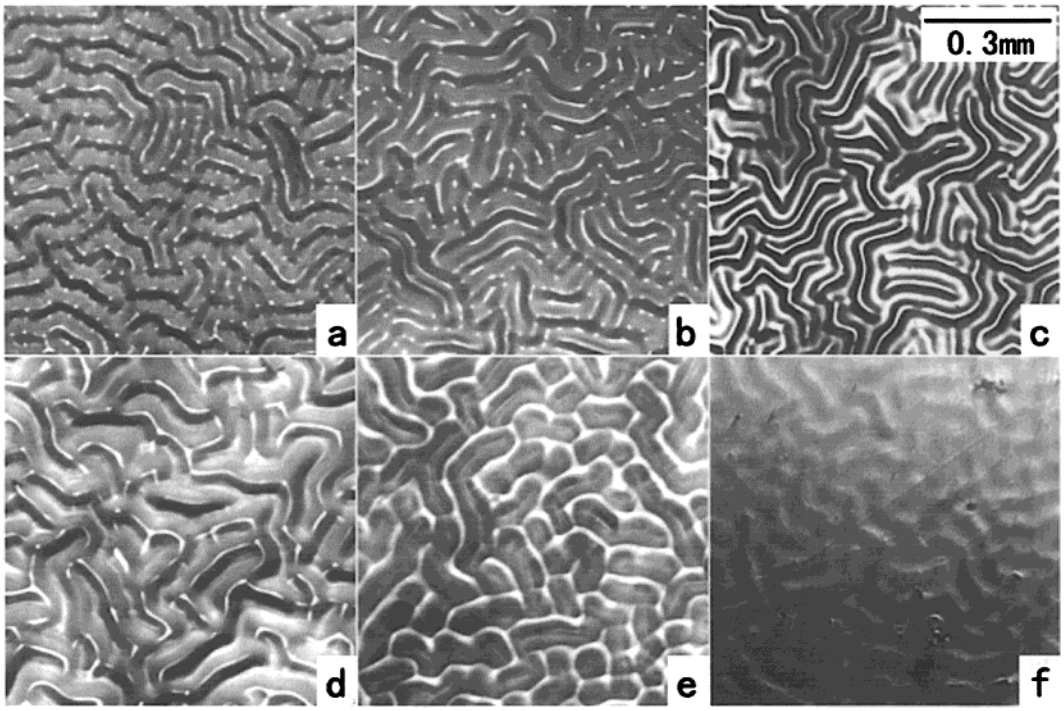

Figure 3. Surface patterns formed on specimens irradiated to 300 kGy at a dose rate of 7.1 kGy/h and immersed in deionized water at 30 °C: (a) 5, (b) 20, (c) 60, (d) 150, (e) 330, and (f) 600 min.

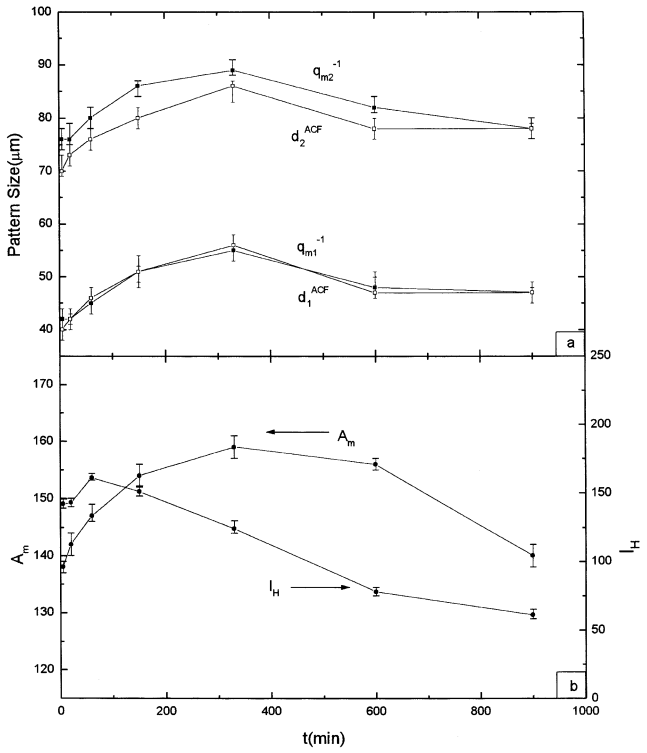

Figure 4. Plot of (a) pattern size and (b) regularity and depth of undulation of pattern on the specimen treated with 300 kGy at a dose rate of 7.1 kGy/h and deionized water at 30 °C vs swelling time.

larger than that of q_{m2}^{-1} and d_2^{ACF} during swelling. That is, the period of short-range structure is more stable than that of long-range structure. On the other hand, the curves of A_m and I_H also display a maximum during swelling.

The pattern size and regularity grow during the initial swelling period due to relaxation of surface constraints with increasing swelling. However, the size and regularity of patterns are influenced by both cross-link density gradients and enhanced swelling due to the radiation-induced formation of carboxylic acid groups.[18,19] Finally, although the pattern is less intense upon the completion of swelling, the size is constant and does not disappear. This trend is different from that observed by Tanaka et al.[1] Their results indicate that the pattern on the swelling gel continues to grow and then disappears at the swelling equilibrium. However, they also found if one side of the sample was fixed by covalently cross-linking it to a film, the evolution of pattern size ceased because of the permanent mechanical constraint. In our case, the pattern arises from a radiation-induced chemical structure gradient, which persists after the swelling process is complete. That is, the inhomogeneous distribution of carboxyl groups and cross-link density induce the permanent mechanical constraint and swelling gradient.

The maximum values of q_{m1}^{-1}, q_{m2}^{-1}, d_1^{ACF}, d_2^{ACF}, A_m, and I_H during swelling of samples irradiated at doses of 100, 200, and 300 kGy are listed in Table 3. The data for 400 kGy were not obtained due to experimentally induced serious surface damage. The maximum values of q_m^{-1} and d^{ACF} during swelling increase with increasing doses. The sample treated with 200 kGy has maximum values of A_m and I_H.

3.4. Effect of Dose Rate on the Pattern Structure. The equilibrium patterns of samples exposed to 400 kGy at different dose rates are shown in Figure 5. Many equiaxed grains are dispersed on the surface. The grain size increases with decreasing dose rate. This is consistent with the interpretation that lower dose rates result in higher carboxylic acid contents and increased molecular weight between cross-links, both of which increase swelling. After image analysis, the curves of characteristic parameters of pattern (A_m, I_H, q_{m1}^{-1}, q_{m2}^{-1}, d_1^{ACF}, and d_2^{ACF}) vs dose rate are shown in Figure

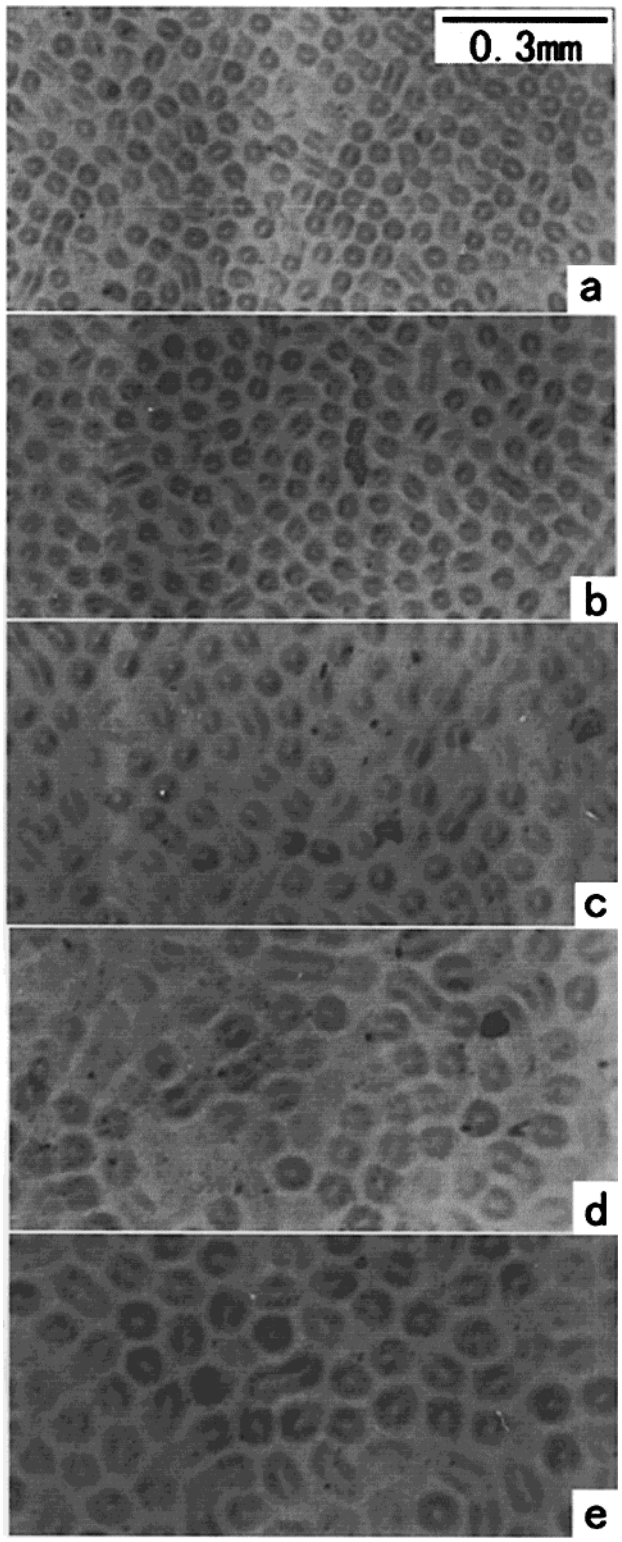

Figure 5. Effect of dose rate on the equilibrium patterns on specimen exposed to 400 kGy and deionized water at 40 °C: (a) 30, (b) 21, (c) 14.5, (d) 10, and (e) 6.5 kGy/h.

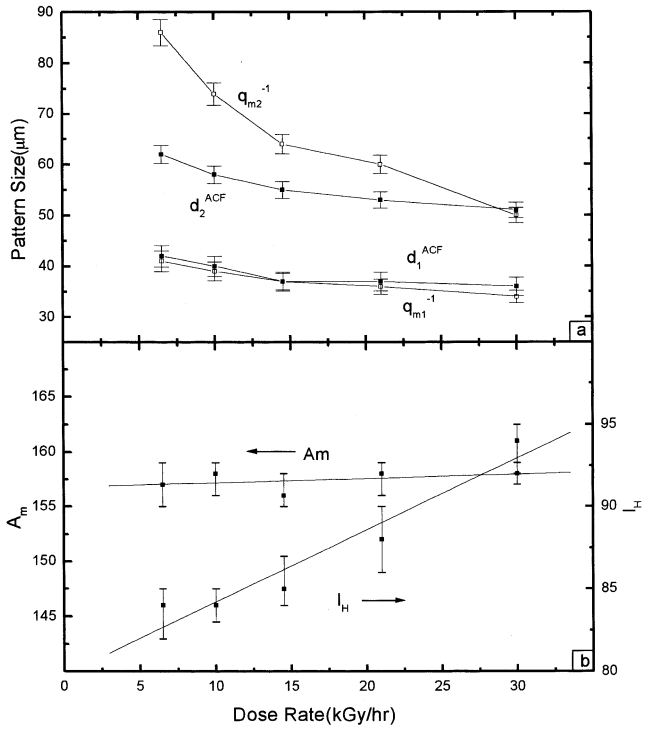

Figure 6. Plot of (a) pattern size and (b) regularity and depth of undulation of patterns on the specimen treated with 400 kGy and deionized water at 40 °C vs dose rate.

6. The values of q_m^{-1} and d^{ACF} increase with decreasing dose rate, while A_m is almost constant. This implies that pattern regularity is independent of the dose rate. I_H increases with the increasing dose rate.

The dose rate follows the probability and depth of oxidation. When the total irradiation dose is constant, the oxidation layers of samples exposed to low dose rates are deeper and more homogeneous than those with high dose rates. Therefore, the patterns on the specimens irradiated at lower dose rates are greater and smoother, but pattern regularity on the samples is nearly constant for all dose rates.

3.5. Effect of pH on the Pattern Structure. The investigation of pH effects verifies our hypothesis on pattern formation on the surface-irradiated polymers. The surface morphology of irradiated specimens immersed in buffer is different from that immersed in water (Figure 7). For the samples treated with 200 kGy, no pattern was observed on the surface of specimens immersed in the solvent at pHs less than 7.2, and many needlelike grains appear if the solvent pH is greater than 7.2. However, if the dose is increased to 300 kGy, an undulation pattern appears on the surfaces of samples immersed in solvents with pH values from 3.9 to 7.8 (Figure 7). The surface morphology exhibits noodlelike grains at low pH values and needlelike grains at higher pH values. Moreover, the surface layer peels off when samples irradiated to 400 kGy are immersed in solutions of pH 7. The species and concentration of ions in the outer layer of irradiated polymers and in the buffer solution environment are different. The great osmotic pressure (due to different concentrations of ions in the surface layer and the surrounding solution) leads to water flow into the specimen, and the specimen expands under extreme swelling when the irradiated specimen with acidic functional groups is immersed in solutions of high pH.[19] The appearance of needlelike patterns is the result of rapid growth of patterns under the high osmotic pressure. Thus, the pattern leaves only the needlelike tip of the surface ridge visible.

4. Conclusions

Buckling patterns develop on the surfaces of polymers irradiated with γ-rays in air and subsequently immersed in water and buffer solutions. The pattern formation is found to be a consequence of the inhomogeneous distribution of carboxyl groups and inhomogeneous cross-link densities induced by oxidation. The structure parameters of patterns, including pattern size, regularity of structure, and depth of undulation, change with swelling time. The patterns continue to grow until the specimens are saturated with water and then persist. Pattern sizes decrease with increasing dose rates. However, the depths of undulation exhibit an

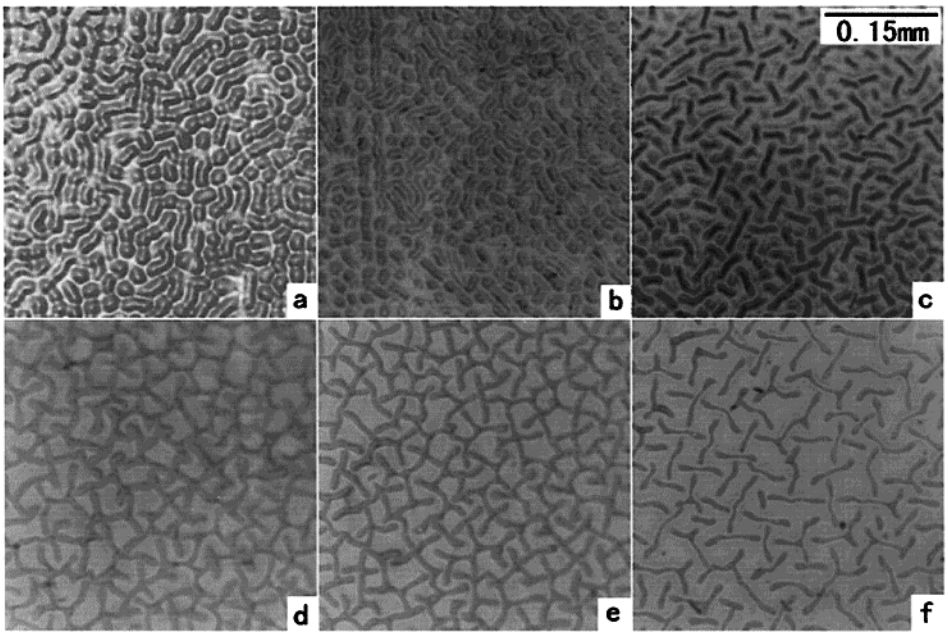

Figure 7. Effect of pH value on the surface patterns of the specimen treated with 300 kGy with dose rate 14.5 kGy/h and immersed in buffer at 40 °C: (a) pH 3.9, (b) pH 4.8, (c) pH 5.6, (d) pH 6.5, (e) pH 7.2, and (f) pH 7.8.

opposite trend. This is due to steeper gradients in radiolysis products produced in lower dose rate experiments. The texture of surface patterns on irradiated polymers changes with the pH environment. All this is indicative of persistent structure-induced gradients in swelling stresses.

Acknowledgment. This work was supported by the National Science Council of Taiwan, Republic of China.

References and Notes

(1) Tanaka, T.; Sun, S. T.; Hirokawa, Y.; Katayama, S.; Kucera, J.; Hirose, Y.; Amiya, T. *Nature (London)* **1987**, *325*, 796.
(2) Hirokawa, Y.; Kucera, J.; Sun, S. T.; Tanaka, T. In *Physical Optics of Dynamic Phenomena and Processes in Macromolecular Systems*; Sedlacek, B., Ed.; Walter de Gruyter & Co.: Berlin, Germany, 1985; pp 197−204.
(3) Sekimoto, K.; Kawasaki, K. *J. Phys. Soc. Jpn.* **1987**, *56*, 2997.
(4) Hwa, T.; Kardar, M. *Phys. Rev. Lett.* **1988**, *61*, 106.
(5) Suematsu, N.; Sekimoto, K.; Kawasaki, K. *Phys. Rev. A* **1990**, *41*, 5751.
(6) Onuki, A. *Phys. Rev. A* **1989**, *39*, 5932.
(7) Panyukov, S.; Rabin, Y. *Phys. Rep.* **1996**, *269*, 1.
(8) Sekimoto, K.; Kawasaki, K. *J. Phys. Soc. Jpn.* **1988**, *57*, 2594.
(9) Panyukov, S.; Rain, Y. *Macromolecules* **1996**, *29*, 8530.
(10) Reiter, G. *Phys. Rev. Lett.* **1992**, *68*, 75.
(11) Reiter, G.; Auroy, P.; Auvray, L. *Macromolecules* **1996**, *29*, 2150.
(12) Redon, C.; Brzoska, J. B.; Brochard-Wyart, F. *Macromolecules* **1994**, *27*, 468.
(13) Van Oss, C. J.; Chaudhury, M. K.; Good, R. J. *Chem. Rev.* **1988**, *88*, 927.
(14) Sharma, A. *Langmuir* **1993**, *9*, 861.
(15) Maldarelli, C.; Jain, R. K.; Ivanov, I.; Ruckenstein, E. *J. Colloid Interface Sci.* **1980**, *78*, 118.
(16) Vrij, A.; Overbeek, J. T. G. *J. Am. Chem. Soc.* **1968**, *90*, 3074.
(17) Sharma, A. *Langmuir* **1993**, *9*, 3580.
(18) Chou, K. F.; Han, C. C.; Lee, S. *J. Polym. Sci., Part B: Polym. Phys.* **2000**, *38*, 659.
(19) Chou, K. F.; Han, C. C.; Lee, S. *Polymer* **2001**, *42*, 4989.
(20) Wallace, J. S.; Sinclair, M. B.; Gillen, K. T.; Clough, R. L. *Radiat. Phys. Chem.* **1993**, *41*, 85.
(21) Gillen, K. T.; Wallace, J. S.; Clough, R. L. *Radiat. Phys. Chem.* **1993**, *41*, 101.
(22) Harmon, J. P.; Gaynor, J. F.; Taylor, A. G. *Radiat. Phys. Chem.* **1993**, *41*, 153.
(23) Bertolucci, P.; Biagtan, E.; Goldberg, E. P.; Schuman, P.; Schuman, W.; Harmon, J. P. *Polym. Eng. Sci.* **1998**, *38*, 699.
(24) Biagtan, E.; Goldberg, E. P.; Harmon, J. P. *Nucl. Instrum. Methods Phys. Res. B* **1996**, *108*, 125.
(25) Biagtan, E.; Goldberg, E. P.; Harmon. J. P.; Stephens, R. *Nucl. Instrum. Methods Phys. Res. B* **1994**, *93*, 296.
(26) Skoog, D. A.; West, D. M.; Holler, F. J. *Analytical Chemistry: An Introduction*, 5th ed.; Saunders College Publishing: Philadelphia, PA, 1990; Chapter 12.

MA021635G